Recent Applications of Aggregation Induced Emission Probes for Antimicrobial Peptide Studies

Tracey Luu,[a] Wenyi Li,*[b] Neil M. O'Brien-Simpson,[b] and Yuning Hong*[a]

[a] T. Luu, Dr. Y. Hong
Department of Chemistry and Physics, La Trobe Institute for Molecular Science, La Trobe University, Melbourne VIC 3086 Australia
E-mail: y.hong@latrobe.edu.au
[b] Dr. W. Li, Prof. N. M. O'Brien-Simpson
Bio21 Institute, University of Melbourne, Melbourne, VIC, 3010 Australia
Centre for Oral Health Research, Melbourne Dental School, University of Melbourne, Melbourne, VIC, 3010 Australia
Email: wenyi.li@unimelb.edu.au

Abstract: Antimicrobial peptides (AMPs) are being intensively investigated as they are considered promising alternatives to antibiotics where their clinical efficacy is dwindling due to the emergence of antimicrobial resistance (AMR). Accompanying with the development of AMPs, a number of fluorescent probes have been developed to facilitate the understanding the modes of action of AMPs. These probes have been used to monitor the binding process, determine the working mechanism and evaluate the antimicrobial properties of AMPs. In particular, with the recent advance of aggregation-induced emission (AIE) fluorophores, that show many advantageous properties over traditional probes, there is an increasing research interest in using AIE probes for AMP studies. In this review, we give an overview of AMP development, highlight the recent progress of using fluorescence probes in particularly AIE probes in the AMP field and propose the future perspective of developing potent antimicrobial agents to combat AMR.

1. Introduction

The discovery of penicillin built a strong foundation for the development of antibiotics to treat bacterial infections[1]. The wide spread adoption of antibiotics with poor treatment management and their use as growth promoters in livestock, has led to the development of multi-drug resistant (MDR) microbes, causing World-wide antimicrobial resistance (AMR)[2] [3]. Horizontal gene transfer of AMR genes across microbial species has facilitated the resistance evolution to a board range of microbes[4]. Currently, antibiotic development is largely focused on modifying the structures of known antibiotics with limited work on developing brand new antibiotics, which, is a reflection on the rapid increase in AMR to clinically approved drugs[5]. With the current COVID-19 pandemic impact, clinical health care center's have been inclined to use more antibiotics to tackle SARS-CoV-2 infectious complications, leading to increased concerns of an uprising of AMR[6].

To resolve the problem of AMR, researchers are developing alternative preventives and therapies, such as phage therapy, lysins, antibodies, probiotics, immune stimulation and peptides[7]. Among them, antimicrobial peptides (AMPs) are emerging as a promising alternative due to their multimodal form of action and a reduced tendency of AMR induction[8]. AMPs are typically short cationic peptides that have a membrane-lytic mechanism induced by self-aggregation and segregation, leading to cytoplasmic leakage and microbial cell death[9]. Up to now, three predominant models are proposed to describe AMP membrane-lytic mechanism: barrel-stave model, toroidal model and carpet model (Figure 1)[10]. From the barrel-stave model, the AMPs bind to the cell membrane perpendicularly to insert into the hydrophobic core of the membrane, associating with each other to cause pore In general, AMR involves changes and adaptations in the bacterial membrane resulting the modulation of antibiotic uptake, modifying the antibiotic and lead to inactivation and efflux[3]. The formation in the membrane. The toroidal model describes the AMPs causing membrane curvature change due to deep penetration into the membrane, disrupting the electrostatic properties, leading to the formation of toroidal shaped pores. Finally, in the carpet model, the cell membrane is covered with a high surface concentration of AMPs, leading to a collapse in membrane integrity.

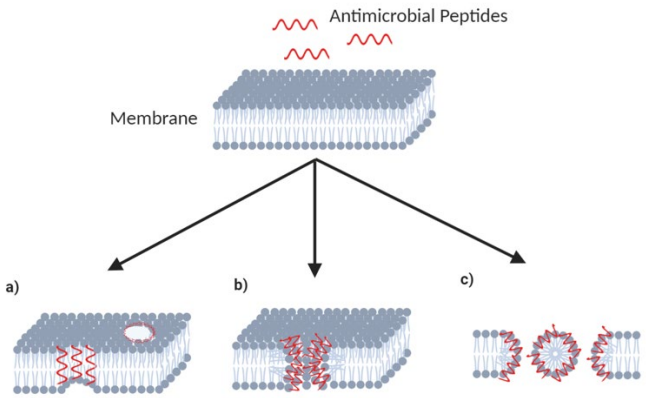

Figure 1. Proposed membrane targeting mechanism of AMPs in a bacterium: the disruption of the membrane induced by self-aggregation and segregation of the AMPs via three main pathways: a) Barrel-stave model, b) Toroidal model and c) Carpet model.

In general, AMR involves changes and adaptations in the bacterial membrane resulting the modulation of antibiotic uptake, modifying the antibiotic and lead to inactivation and efflux[3]. The membrane disruption property of many AMPs has been shown to be highly effective against Gram-negative bacteria as well as Gram-positive bacteria with the mechanism of action been shown to be multi-modal[11]. This ability of AMPs of physically disrupting the bacterial membrane, is one possibility why bacteria have a reduced tendency of developing resistance to AMPs[9]. Recently, there is an increasing number of AMPs entering clinical trials[10c, 12], showing the promise of AMPs in therapeutic application. Tremendous research efforts have been devoted to enhance the bioactivity of AMPs, which are summarized in several recent review articles[13]. With the increasing number of publications on AMPs and their important therapeutic promise, it is important to understand and investigate the specific mechanisms of different peptides for the future development and rational design of AMPs.

Currently, there are a limited number of technologies available for the study and visualization of AMPs' membrane disruption mechanisms, these include solid-state nuclear magnetic resonance (NMR) spectroscopy[14] and X-ray crystallography[15]. Unfortunately, these techniques such as NMR spectroscopy, have an inherently low sensitivity and thus require a larger amount of sample in comparison to other techniques[16]. The process of crystallization is challenging or not currently possible for X-ray crystallography of an AMP in a lipid/hydrophobic environment to generate static three-dimensional images[17]. Although advances in solid state NMR have meant that AMP interaction with a whole bacteria can be monitored[18], it is limited by the accessibility and complexibility. Thus, there is limited knowledge on how AMPs are internalized in bacteria[19] and few tools available for thorough examination of the localization of AMPs in bacteria[20]. On the other hand, fluorescence-based technologies are found to be effective tools for the study of such dynamic events in real time using bacteria. The use of a sensor or a probe to generate fluorescence signals, the binding process of AMPs to bacteria and their real time locations inside the bacteria can be monitored with suitable resolution of microscopy[21]. Furthermore, fluorescence has also been used to detect the antibacterial properties of AMPs, allowing better determination of their potency and efficacy, resistance state, toxicity levels and mode of action in a high-throughput manner[22].

However, most of the conventional organic fluorescent probes used in these studies have been found to self-quench when they are placed under higher concentration, resulting in lower fluorescence intensity[23]. This effect is known as the aggregation-caused quenching (ACQ) effect[23]. The ACQ effect has been used in some applications such as in calcein leakage assay[24] to determine the model membrane lysis in the presence of AMPs. However, in many scenarios, the ACQ effect hampers the applications of the fluorescent probes especially in aqueous media when hydrophobic dye molecules with planar disc like structures tend to aggregate and form strong π-π interactions that quench fluorescence. To overcome the issue of ACQ, Tang *et al* developed a new class of fluorescent materials possessing the opposite effect[25]. These materials, namely aggregation-induced emission (AIE) fluorophores, are virtually non-emissive when molecularly dissolved in good solvents but become highly fluorescent in their aggregate or solid state[26]. Most of the AIE fluorophores possess a twisted propeller conformation that can actively undergo intramolecular motions when photoexcited in solution to diminish the fluorescence. In the aggregate or solid state, such intramolecular motions will be restricted while the twisted structure also prevents the strong π-π interactions[26]. Therefore, a strong fluorescence can be observed when AIE molecules aggregate. Typical AIE molecules include tetraphenylethene, tetraphenylsilole, quinoline-malonitrile, cyanostilbene, 9,10-distrylanthracene and organoboron complexes[27].

The AIE phenomenon can thus be modulated based on the restriction of intramolecular motions, which can be adapted as a unique strategy for designing fluorescent sensors. The biological substance is required to interact noncovalently or covalently with the AIE molecules. Currently, there are four main AIE-based strategies for the detection of biological substances: i), encapsulation or ligand-type binding at the pockets, ii), targeted ligand-guided interactions, iii), reaction-based conjugation and iv), aggregation/disaggregation-driven mechanism by the biological target[28]. In comparison to conventional fluorescent, fluorophores with AIE characteristics showed many advantages including high resistance to photobleaching, high performance in long term real-time monitoring, and are cost-effective to synthesize[29]. In general, the AIE probes can serve as a good alternative to conventional fluorophores with the possibility of overcoming some challenges of other fluorescence probes for biosensor and bioimaging. So far, the AIE probes have been broadly applied in many areas to analyze important biological substances *in vitro*, *in vivo* and in body fluids[30].

The number of publications on AIE and using AIE luminogens in the antibacterial field has been increasing especially since 2016 (Figure 2), indicating the growing interest of integrating AIE with antibacterial research. However, there is a lack of a summary and perspective of using fluorescent probes to assist in the development of AMPs. Therefore, in this review, we will first summarize the recent research progress of AMPs focusing on those used in clinical trials and in veterinary and food industry, followed by a focus on using traditional and AIE probes in assisting our understanding of AMPs mechanism of action. The comparison of traditional fluorescent dyes and AIE dyes in current AMP applications, as well as the perspective of AIE probes for AMP development will be further highlighted.

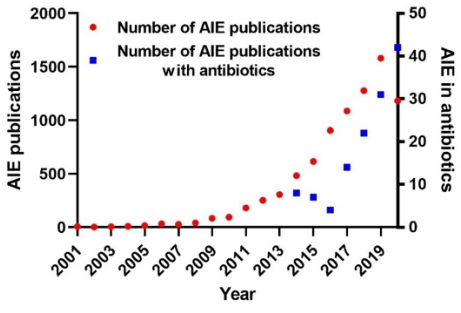

Figure 2. The number of publications each year of AIE (red) and AIE in antibiotics related research (blue) from 2001 to 2019. The counts were collected from SciFinder using the keywords ("Aggregation-induced emission" for AIE data collection; "Aggregation-induced emission" in "antimicrobial", "antibacterial", or "antibiotic" for AIE in antibiotics data collection).

2. Current AMP applications

Since AMPs have been shown to be a promising candidates to traditional antibiotics, they have been applied to many applications of interest including in drug development[31], immune-stimulation[32] and other biological and biomedical areas[33]. In this section, we will briefly introduce several selected AMPs that are in clinical trials, as potential therapeutics and in veterinary and food industry applications.

2.1. AMPs in Clinical Trials

With an increasing research and development focus on AMPs, there are a growing number of AMPs entering pre-clinical and clinical trials[34], with 27 AMPs entering phase I-III clinical trials up to 2018 [10c]. As previously mentioned, many of the clinical AMPs are reported to have a direct antimicrobial activity through the bacterial membrane disruption mechanism. In this section, we will introduce and discuss representative AMPs that are in clinical trials including iseganan (toroidal model), brilacidin (carpet model) and DPK-060 for topical, oral and intravenous treatments, respectively (Figure 3).

Iseganan was submitted for the treatment of oral mucositis in patients with head and neck cancer and was tested up to phase III clinical trials[35]. This AMP is derived from protegrin-1 was shown to have a toroidal pore formation mechanism for membrane disruption[36]. During the early development, it displayed a broad and rapid bactericidal activity with a lack of observed resistance and high stability in biological fluids. Iseganan was found to be well-tolerated after oral administration during phase II study[37] and patients felt less pain while being under iseganan treatment. However, in phase III trial it was terminated since as it showed low effectiveness as a treatment for oral mucositis[37]. Although terminated, the trial data suggested iseganan has application for future development. Recently, Polyphor Ltd. has started to use an iseganan derivative called murepavadin, which has shown promising results in targeting *Pseudomonas aeruginosa* lung infections in patients with cystic fibrosis[38]. It is currently registered for its first-in-human clinical trial via an oral inhalation route (Polyphor Ltd IN December 2020).

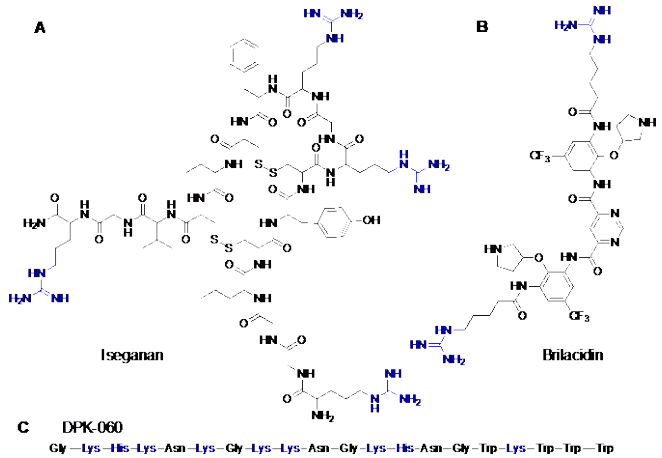

Figure 3. Chemical structure of A) Iseganan and B) Brilacidin and C) amino acid sequence of DPK-060. The positively charged side chains are highlighted in blue.

Another AMP termed brilacidin is currently being tested for a number of disease conditions including patients with oral mucositis[39], patients with ulcerative proctitis and patients with acute bacterial skin and skin structure infection (ABSSSI)[40]. It has been demonstrated that brilacidin disrupts bacterial membrane by the carpet pore formation mechanism[41]. Brilacidin is found to be advantageous in many situations to kill antibiotic sensitive and MDR bacteria and prevent resistance development[42]. For the treatment of ABSSSI, a single intravenously-administered dose was found to be effective, generally safe and well-tolerated[40]. Furthermore, a direct comparison of brilacidin with a 7-day regimen of the FDA-approved lipopeptide antibiotic Daptomycin, found that it had equivalent efficacy[42]. More recently, brilacidin entered phase II clinical trial studies as a potential COVID-19 treatment as it was shown to disrupt viral integrity and inhibit viral entry[43]. In initial studies, it has shown to be effective against different SARS-COV-2 strains *in vitro*, indicating the possibility of using this AMP for overcoming emerging COVID-19 mutations. Thus, it showcases the potential applications of AMPs in treating not only bacterial infection but various diseases by direct/indirect pathways.

DPK-060, an AMP developed by DermaGen AB and Promore Pharma (formerly Pergamum AB), is currently under clinical trial for the treatment of skin infections[44]. Due to its highly charged structure (net charge +8.5 at pH 5.5), DPK-060 exhibits various membrane disruption mechanisms including negative curvature of pores, membrane thinning or local packing defects[45]. These suggested that additional membrane disruption strategies may be adopted by AMPs that further lead to membrane lysis. DPK-060 itself shows a broad spectrum of antimicrobial activity and thus can be applied to many types of skin infections. It has been shown that DPK-060 can withstand the *in vivo* enzymatic degradation, thus increasing its bio-availability in the body[44]. The prolonged *in vivo* circulation lifetime showed no signs of cytotoxic effects, which further suggests it as a promising AMP candidate. During the phase II clinical trial, it was delivered topically in an ointment and shown to have high efficacy and safety margins. The topical treatment was well tolerated by the patients and they had a decrease in the microbial density in eczematous lesions. These outcomes indicated the potential of DPK-060 as a topical treatment of skin microbial infections. However, to ensure that the results maintain the efficacy and safety levels, a longer follow-up period is still required to move onto the next phase of clinical trials.

In summary, there are a number of AMPs that are currently under clinical investigation with different forms of delivery including topical, oral and intravenous for different diseases. It indicates the promise of AMPs as potential therapeutics for different treatment applications and the examples here highlight that an understanding of the mechanism of action is an important feature of AMP clinical development.

2.2. Enhancing delivery of AMP Therapeutics for a Broad Range of Infections

The significant potentials of AMPs over conventional antibiotics have led many applications in treating infections associated with many conditions including metabolic, cardiovascular and oncology diseases[12]. AMPs analogues can be readily produced by using peptide synthesis strategies, which can then be adapted for enhanced delivery packages to the site of infection. Two extensively studied peptide polymyxin E (colistin) and LL-37 have been adapted to enhance their efficacy with different delivery strategies[46] Due to the broad spectrum in treating different infections[47], we highlight the current strategies in using these peptides (Figure 4B & D) as potential therapeutics.

Due to the molecular size, the delivery of peptide drugs to the targeted area is a major challenge in AMP development[48]. Recent studies highlighted that such an issue can be overcome by incorporating modern nanotechnologies. For instance, Uttley *et al* used cationic peptide antibiotic, colistin, to target the MDR *Pseudomonas aeruginosa* strains in lung infections of cystic fibrosis patients[49]. However, due to its positive charge, colistin as well as interacting with the bacterial biofilm also strongly interacts with the airway mucus thus, decreasing its availability to reach and treat the bacterial biofilm at the infected site[49]. The development of nanoparticle delivery was able to overcome this boundary of using free peptide molecules by encapsulating them in a nanomaterial to increase its delivery and enhance the therapeutic efficacy[50]. d'Angelo *et al*[51] engineered a nanoparticle platform for local delivery of colistin (Figure 4A). By encapsulating the cationic peptide in poly lactic-co-glycolic acid (PLGA), it helped increase the bio-availability of peptide to reach the targeted site, as well as prolonged its residence time (half-life) and thus, decreased the number of administrations required to attain efficacy. By using chitosan on the surface of the nanoparticle, it promoted colistin diffusion through artificial mucus and thus, improved the transportation of the nanoparticle to the target site.

A similar approach has been used for treatment of diabetic wound healing, which is a major complication with no effective therapy for diabetes[52]. Impaired angiogenesis and bacterial infection are the main causes preventing diabetic wound healing[53]. The AMP, LL37, originated as a treatment for chronic leg ulcers[54], and is reported to have a toroidal pore mechanism of action which enhances its bacterial cell penetration properties[55]. Wang and co-workers have reported a novel gene delivery strategy of coupling LL37 and pro-angiogenic plasmid DNA with a grafted ultra-small gold nanoparticle (~10 nm in diameter) as a topical treatment of diabetic wounds (Figure 4C)[56]. They showed that this hybrid nanoplatform can not only maintain the highly antibacterial activity of LL37 (Figure 4E), but also enhance the cellular and nucleus uptake of the gold nanoparticles to achieve a high gene delivery efficiency. Due to this synergistic effect, this AMP-DNA nanoparticle inhibited the bacterial infection on the diabetic wound and resulted in a faster wound closure rate. Furthermore, there was no significant damage to the main organs after treating the wound, indicating low cytotoxicity and biocompatible of the LL37 loaded gold nanoparticles.

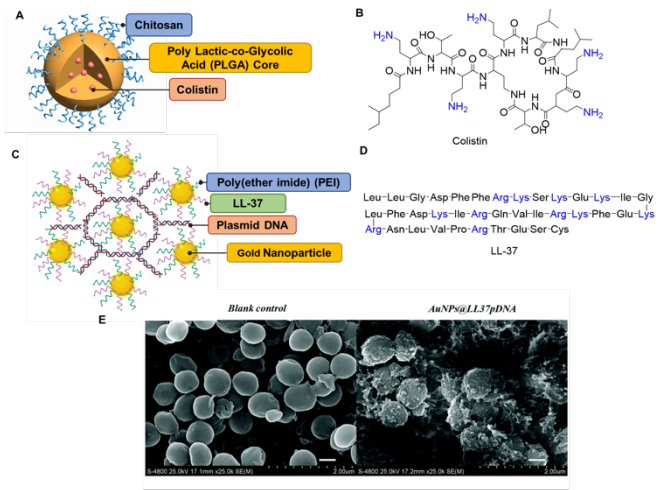

Figure 4. A) Nanoparticle structure of Colistin-Chitosan complex. B) Chemical structure of colistin. C) Schematic diagram of gold nanoparticles with poly(ether imide), LL-37 and plasmid DNA. D) The sequence of LL-37. E) Representative SEM micrographs of bacteria before and after incubation with AuNPs@LL37/pDNAs. Scale bar: 4 μm. Reproduced from Ref. [56] with permission from The Royal Society of Chemistry.

Both examples demonstrated the promise of engineering nanoparticles to improve the delivery of AMPs to the desired site prior to the loss of pharmacological effects, as well as to improve the efficiency of AMPs for treating infections associated with other disease conditions in clinical settings *in vivo*. Critical in their development was the peptide loading and monitoring of the peptide-nanoparticle delivery to the bacterial sites. AIE has been extensively used to monitor both peptide and drug loading on to nanoparticles and localize these materials to the site of interest such as certain organelles in cells and tumor region *in vivo*[57] but has been underutilized in the field of AMP delivery.

2.3. AMPs in Veterinary and Food Industry

In addition to human antibacterial drug development, there has been an increasing number of AMP publications and patents in the veterinary and food industry over the years (Figure 5). AMPs have been reported to be highly effective against plant microbes, food-contaminating organisms and insect pests[58]. In this section, we highlight three AMPs applied in the treatment of veterinary diseases, food preservation and food processing (Table 1).

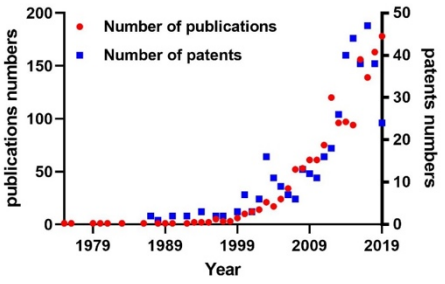

Figure 5. The number of publications (red) and patents (blue) of AMPs each year reported in the agriculture/food industry/veterinary research field until 2019, collected from SciFinder using keywords ("antimicrobial peptide", "antibacterial peptide", or "host defense peptide" in "agriculture", "food industry" or "veterinary").

In the veterinary field, AMPs have been reported to be used to treat bacterial infections in livestock and pets. Recently, Jarosiewicz and co-workers tested a number of AMPs[59] including Uperin 3.6 against Coagulase-positive *staphylococci* (CoPS) (Table 1)[60], which are predominant pathogens present in canine skin infections[61]. Due to antibiotic resistance bacteria, these conditions tend to recur and thus AMPs have great potential as an alternative to conventional antibiotics for treating skin infections. Interestingly, the tested AMPs exhibited equal efficiency against MDR strains and antibiotic susceptible strains. Furthermore, these AMPs showed higher effectiveness against the very common canine disease causing bacteria *S. pseudintermedius* in comparison to *S. aureus* strains. Overall, this study showed encouraging results of using AMPs as a potential therapeutic to overcome AMR in treating canine pyoderma.

Table 1. Representative AMPs used in veterinary and food industry.

AMP name	Sequence
Uperin 3.6	H-GVIDAAKKVVNVLKNLF-NH_2
1018K6	H-VRLIVKVRIWRR-NH_2
cLFchimera	H-DLIWKLLVKAQEKFGRGKPSKRVKKMRRQWQACKSS-NH_2

In the food industry, food packaging is essential as a protective barrier to preserve food quality. In recent years, the incorporation of AMPs into food packaging has been shown to have significant social and economic impacts for food bio-security[62]. For example, AMP 1018K6 has been conjugated to polyethylene terephthalate to produce packaging material that showed high antimicrobial and antibiofilm activity (Table 2)[63]. The results showed that food packaging material containing the AMP reduce the number of bacteria, yeast and mold spoilage in dairy products. Further, it was shown to be effective against *Listeria monocytogenes*, a foodborne pathogen, and inhibited its biofilm formation. These results demonstrate the diverse application of AMPs in inhibiting bacteria growth in packaged food, which can potentially increase packaged food shelf-life.

A major issue in food processing facilities is the difficulty of removing bacterial biofilms from processing equipment using clinical antibiotics, thus contaminating food packaging with foodborne pathogens. Taehaeian and co-workers have recently reported an effective method to remove bacterial biofilms to allow safe food production by using a chimeric form of an AMP derived from lactoferrin, termed cLFchimera (Table 2)[64]. Using genetic engineering approach, *Lactococcus lactis* (a food grade bacteria considered as safe additive in dairy products for gastrointestinal tract disorder[65]) was used to express and secrete cLFchimera into the culture medium, which is found to have remarkable antibacterial activity against different foodborne pathogens[66]. Interestingly, this AMP also showed anti-biofilm formation and antioxidant activity, indicating that inclusion of this new bacterial strain in food would be able to remove the biofilm but also be safe to use in oral consumption. With the promising use as a food preservative in dairy products, more in-depth study would be required to evaluate its safety and efficacy before the application of this AMP in the food industry. One way to conduct in-depth studies, including measuring the release kinetics of the AMP and its half-life, is to use fluorescent dyes, such as AIE fluorogens to observe its mechanism due to its easy use and practicality.

3. Use of Traditional Dyes in Antimicrobial Applications

With the promising outcome of employing AMPs in a variety of applications, it is fundamentally important to understand the working mechanism of an AMP in order to manipulate their biological activities and improve efficacy. Among different biophysical and biochemical techniques, fluorescence-based techniques have been widely employed for such purposes with easy accessibility and high throughput capability. In general, fluorescent labelled AMPs are used for real-time analysis to monitor AMP behaviors and interaction processes. However, the direct conjugation of fluorophore to short AMPs is deemed a challenge as the conjugation of a fluorophore may change the charge distribution, hydrophobicity and amphipathicity of the AMP, thus leading to a partial loss of its biological activities[67]. Therefore, the labeling position of the fluorophore needs to be carefully chosen to maintain the bioactivity of the peptides. In this section, we will introduce several of the latest developed strategies for incorporating fluorophores into AMPs whilst retaining their antimicrobial activity. The examples chosen signify well-known traditional dyes used to help with the detection of representative AMPs.

In 2016, Mendive-Tapia *et al* reported a synthetic fluorogenic amino acid building block, Trp-BODIPY, by directly coupling BODIPY to the indole group of tryptophan (Trp)[67a]. Trp-BODIPY is only fluorescent in a hydrophobic environment. They have used Trp-BODIPY as a fluorogenic substitute of Trp in Peptide Anti-Fungal 26 (PAF26) (Figure 6A), which is a synthetic hexapeptide with high selectivity to fungal cells over bacterial and mammalian cells. The resultant peptide maintained its high affinity and selectivity towards fungal cells as revealed by high fluorescence observed on the wash-free imaging of several fungal strains (Figure 6B) but not for human lung epithelial cells in the co-culture system. It suggests a new strategy of incorporating fluorogenic amino acids into AMPs by solid-phase peptide synthesis (SPPS) for real-time study of the affinity and specificity of peptide-targets interaction.

Akram *et al* have described an environmentally-sensitive fluorophore, NBD, labelled AMP, ubiquicidin (NBD-UBI) for *in vitro* detection of bacteria (Figure 6C)[68]. In a separate study, a multivalent approach was used the enhance membrane pore formation and interaction of AMPs to improve antibacterial efficacy[70]. This was then further developed in a novel approach based on a multivalent (tri-branched) form, named NBD-UBI_{dend}, in which the three arms of the trivalent scaffold were all capped with NBD that are self-quenched in aqueous media but become fluorescent after entering into the hydrophobic environment of the bacterial membrane. In addition, the metabolically labile methionine was also replaced with a norleucine analogue in NBD-UBI_{dend}. The conjugates had an enhancement in fluorescence intensity, allowing rapid detection of a broad range of pathogens with high signal-to-noise ratio over the host cells. In comparison to the monomeric NBD-UBI, they further demonstrated that the trivalent scaffold for NBD-UBI_{dend} had enhanced stability in a proteolytic cellular environment and in the presence of surfactants. The trivalent NBD analog retained the high affinity to detect bacteria in situ in the infected explanted human lung model (Figure 6D). Therefore, this study demonstrated that a rational design, utilising fluorophores, as the scaffold may improve the *in vivo* susceptibility of AMPs for clinical utility.

Apart from real time detection of AMPs in cells, tissues and organs, fluorescence can also be a powerful tool to investigate and demonstrate the mechanism of action of AMPs. For example, Gan *et al* had constructed a peptide dendrimer, G3KL, labelled with fluorescein or dansyl, to study its antibacterial mechanistic behaviors[69] (Figure 6E). In combination with super-resolution imaging by stimulated emission depletion microscopy, time-lapse imaging and transmission electron microscopy (TEM), such fluorophore labelled method has been demonstrated to validate that G3KL can selectively accumulate and disrupt the integrity of the outer membrane of Gram-negative bacteria, depolarize the inner membrane and then penetrate into the bacteria (Figure 6F). They further demonstrated that G3KL can bind to endotoxin lipopolysaccharide (LPS), deactivate LPS and inhibit the LPS induced release of pro-inflammatory cytokines such as TNF-α from macrophages. Their study showed the attachment of fluorophore enables the investigation of the detailed mechanism of the AMPs.

However, given the antimicrobial application described in section 3, the use of conventional fluorophores to investigate general biological studies is limited by several factors. First, for some of the fluorophores such as fluorescein, the fluorescence is already on before binding to the target. In that case, careful washing of the unbound fluorophores is necessary to remove the background to improve the signal-to-noise ratio. Secondly, the self-quenching effect caused by increased level of local concentration often leads to the lower fluorescence when binding to biological substances or formation of aggregates. It is also found that the poor photostability of conventional fluorophores causes the loss of its recognition capabilities. Thus, this brings forth the limitations of using traditional dyes and restricting their capability to be a productive quantitative imaging tool for wider applications.

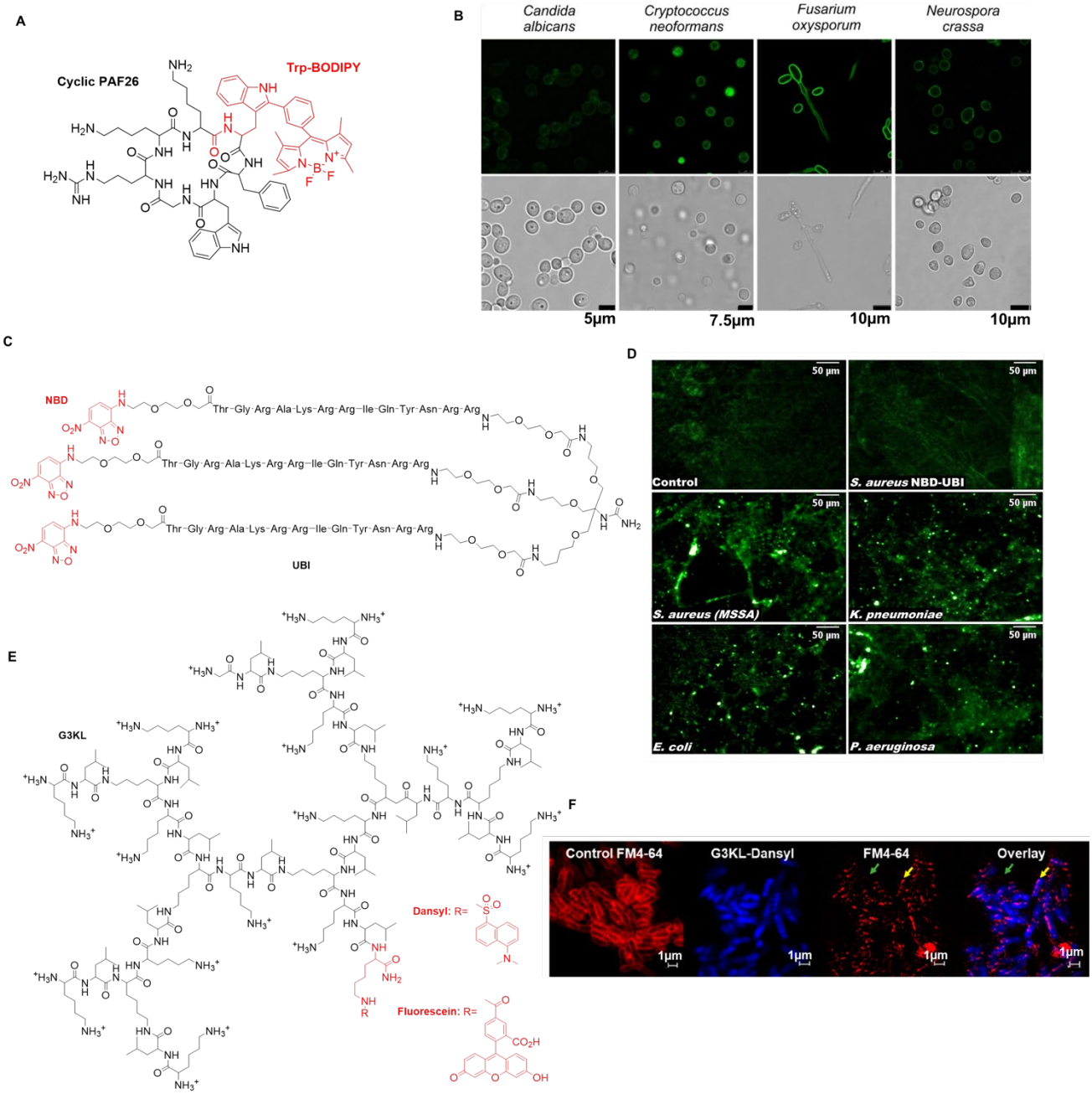

Figure 6. A) Chemical structure of cyclic BODIPY-labelled PAF26. B) Live confocal microscopy of different fungal species with cyclic BODIPY-labelled with fluorescence (top) and brightfield (bottom). (Reproduced from Supplementary Figure 14 of ref [67a]). C) Chemical structure of NBD-UBIdend. D) OEM images of PBS and S. aureus with NBD-UBI, and *S. aureus, K. pneumoniae, E. coli* and *P. aeruginosa* with NBD-UBIdend. (Reproduced from Supplementary Figure 14 of ref [68]) E) Chemical structure of G3KL-Dye. F) Confocal microscopy of *P. aeruginosa* incubated with FM4-64 and treated with G3KL-Dansyl, represented by yellow arrow (structure outside of bacteria) and green arrow (dispersed dye marking the broken membrane). Reprinted (adapted) with permission from ref [69]. Copyright (2019) American Chemical Society. For chemical structures: Red is the Dye and Black is the AMP.

4. Use of AIE Dyes in AMP Studies

To overcome the limitations of traditional dyes described in section 3, AIE dyes are able to improve the feasibility of fluorescence as a quantitative imaging tool. Table 2 summarizes the pros and cons of using AIE probes in comparison with traditional fluorescent probes. Shown in Table 2, AIE dyes are well known for their selectivity, low synthesis cost and enhanced photostability. However, the use of AIE dyes in biological detection are limited by their requirement of a higher concentration in comparison to conventional dyes. Typically, a conventional dyes' concentration can be as low as being in nanomolar while AIE dyes will have concentrations in micromolar[30a, 71]. By having a higher concentration, AIE initiates an easy formation of aggregation, allowing it to be emissive. On the other perspective, due to AIEgen's fluorescence capability in aggregates, it can be easily applied to a wider application[72]. This is demonstrated in Figure 7, where the fluorescence of ACQ and AIE are compared under different water fraction[73].

Table 2. Summary of the strength and limitations of traditional and AIE probes.

	Traditional Dyes	AIE Dyes
Strength	High fluorescent quantum yield in dilute solution	High fluorescence quantum yield in aggregated/solid state
	Large extinction coefficient	Large Stokes shift
	Chemically stable	Chemically and photo-stable
		Highly resistant to photobleaching
		Suitable for long-time tracking
		Relatively easy to synthesize
Weakness	Weakly fluorescent when aggregated	Relatively small extinction coefficient
	Small Stokes shift and self-absorption	Higher concentration usually required
	Fluorescence quenching and photo bleaching	Limited options for water soluble dyes
	Can be difficult to synthesize	

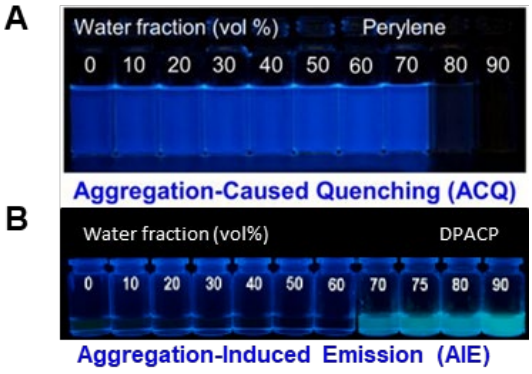

Figure 7. Fluorescence of a) ACQ dye (perylene) in THF/water mixtures with different water content. B) AIE dye (7-(diphenylamino) coumarin-4-yl pivalate/ DPACP) in acetonitrile/water mixtures with different water content. Reproduced with permission from ref [74] with permission from copyright (2015) American Chemical Society and Elsevier.

Due to the advantages highlighted in Table 2, in the past few years, an increasing number of AIE probes have been designed and applied for the detection, identification and treatment of pathogenic infections. A recent review published by Tang and co-workers have nicely summarized the latest development of AIE-active probes and photosensitizers for microbial detection and antimicrobial treatment[75], which is complement with this review of the AIE for AMP mechanism studies. The AIE dyes have been proven to be excellent tools in studying drug/peptide applications on a range of pathogens including bacteria, fungi and viruses. In this section, we will focus on the AIE dyes reported for AMP studies with emphasis on using AIE dyes for the mechanistic investigation of AMPs, as well as a comparison of conventional dyes and AIE dyes for common AMP studies.

4.1. Comparison of AIE and conventional dyes in biological studies

A few studies have compared the efficiency of AIEgens and conventional fluorescent in the biological applications. For example, in 2013, Li *et al* successfully developed AIE dots for non-invasive cell tracing[76]. The Tat-AIE dots, made up of 2,3- bis(4- (phenyl(4- (1,2,2- triphenylvinyl)phenyl)amino)phenyl)fumaronitrile (TPETPAFN), poly(ethylene glycol) (PEG) and PEG-NH_2, were functionalized with cell penetrating peptides, Tat, derived from HIV-1 transactivator of transcription protein to allow for high emission efficiency, strong photobleaching resistance and long monitoring system. This is found to be an improvement to current fluorescent genetic cell tracing since there are limitations to its use including its poor photostability, low efficiency and disrupting normal cell function (Figure 8 A&B)[77]. It was further proven when the Tat-AIE dots were compared to commercially available quantum dots, Qtracker ® 655 under similar conditions. From the results, the Tat-AIE dots indicate an order of magnitude brighter, have excellent fluorescence stability even after 9-day incubation (Figure 8C). Though Qtracker ® 655 are typically used for long-term fluorescent tracing probes, this study suggested the huge potential and advantage of using AIE dots in comparison to the Qtracker ® 655.

Similarly, Sheng and co-workers have used nanoparticles with AIE for cell tracing (Figure 8D&E)[78]. In this study, they have improved the near infrared-II (NIR-II) fluorescence used to image brain tumours by using AIE characteristics rather than ACQ characteristics. NIR-II brings forth deeper penetration and higher spatiotemporal resolution[79], making it an excellent tool to use for brain imaging. However, most NIR-II fluorescence are inorganic[80]. The ones that are organic are typically placed in polymer matrices to increase its biostability and tumour targeting capabilities[81]. However, due to ACQ effects, there is a weakened fluorescence when placed inside nanoparticles. Thus, Sheng *et al* developed NIR-II with AIE in nanoparticles for enhanced brain imaging called TB1 dots[78]. From their results, TB1 has shown enhanced fluorescence quantum yield with a large absorptivity, allowing it to also facilitate NIR-I photoacoustic imaging, which is a much deeper penetration than NIR-II fluorescence. To allow TB1 to target specific tumours, TB1 was covalently grafted with tumour-specific c-RGD peptide. This helped increase its specificity and sensitivity, allowing an accurate assessment of the depth of the tumour inside the brain tissue. Thus, TB1-RGD dots showcases improvement to current organic NIR-II fluorescent nanoparticles with the potential to monitor and visualize the brain tissue.

Additionally, a peptide-conjugated AIEgen (FC-PyTPA) is presented as a multiple agent therapy probe (Figure 8G)[82], which can self-assemble after the addition of siRNA to become FC_{siRNA}-PyTPA. It is found that FC_{siRNA}-PyTPA can respond to the extracellular MMP-2 and lead its cleavage. Once cleaved, PyTPA is able to be internalized in the cells allowing inhibition of tumour growth while FC_{siRNA} enters the cells, form nanofiber which destroys the lysosomal structure and thus siRNA is able to escape. From the results, they have also showed that the AIE probe, PyTPA, gave a higher mean fluorescence intensity in HeLa cells than the conventional dye, Cy5 (Figure 8H). This is found to be useful for image-guided photodynamic therapy, as it helped determine the importance of MMP-2 in improving the cellular internalization efficiency, as well as producing intracellular reactive oxygen species (ROS) to effectively inhibit tumour growth.

Chen et al have found an AIE probe, named AIE-Mito-triphenylphosphonium (AIE-Mito-TPP) (Figure 8I), that is able to image and kill bacteria and cancer cells (Figure 8J)[83]. The AIE-Mito-TPP can quickly kill both Gram-positive and Gram-negative cells via membrane permeability, as well as kill cancer cells by disrupting mitochondrial functions. In comparison with ACQ-active fluorophore, rhodamine, the AIEgens had a better signal-to-noise ratio and a long-term retention inside the bacteria without the need to have a washing step, indicating its promising ability as a bacterial probe. For its antibacterial activity, it has shown to have lower minimum inhibitory concentrations for both Gram-positive and Gram-negative cells than traditional antibiotics and antibacterial agents. Overall, AIE-Mito-TPP provides an efficient method over traditional dyes in monitoring the bacterial killing process *in situ*.

In summary, as an aggregated ensemble, the AIE molecules exhibit enhanced fluorescence intensity that allows high signal-to-noise ratio, extraordinary photostability that provides the opportunity for quantitation and long-term real time *in situ* tracing and other effects, for example enhanced ROS generation capability that are not observed in single molecules. These properties strengthen the use of AIE dyes to overcome challenges faced by traditional fluorophores for mechanism studies in biological systems.

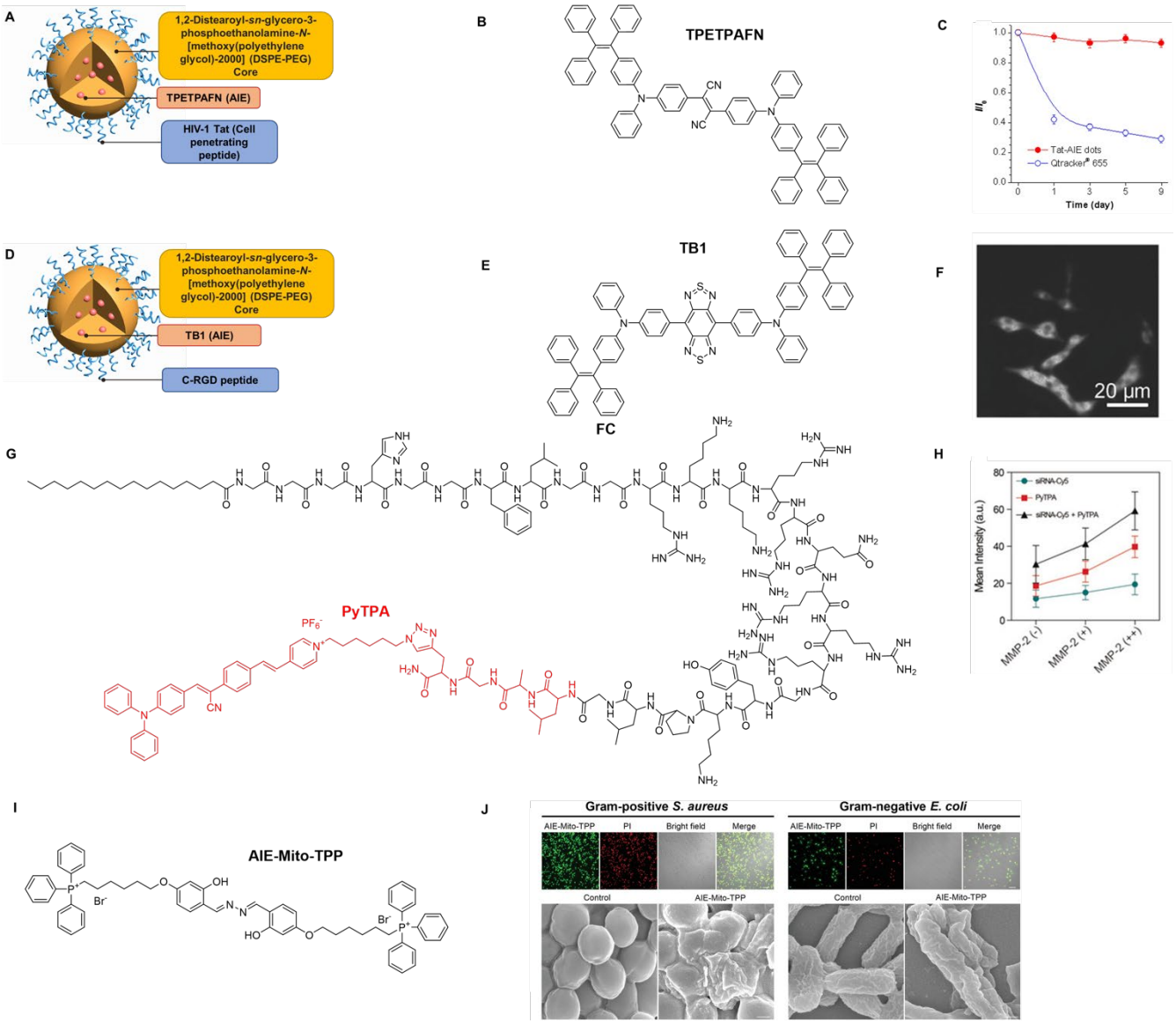

Figure 8. A) Nanoparticle structure of Tat-AIE dot. B) Chemical structure of TPETPAFN; C), Graph of time against PL intensity changes of 2nm Tat-AIE dots and Qtracker ® 655 in Dulbecco's Modified Eagle Medium with 10% fetal bovine serum at 37ºC. Reproduced from ref [76] with copyright from Springer Nature. D), Nanoparticle structure of TB1-RGD dot. E), Chemical structure of TB1. F) NIR-II fluorescence image (1000LP and 10ms) of U87 cells treated with TB1-RGD dots. Reproduced from ref [78]. G) Chemical structure of FC_{SiRNA}-PyTPA. H) Mean fluorescence intensity of HeLa cells treated with PyTPA, Cy5 and $FC_{siRNA\text{-}Cy5}$-PYTPA (5μM). Reproduced from ref [82] I), Chemical structure of AIE-Mito-TPP. J), CLSM images of gram-positive *S. aureus* and gram-negative *E. coli* with AIE-Mito-TPP for 30 mins and stained with PI for 10 mins. [AIE-Mito-TPP] = 5μM, [PI] = 3ug/mL, scale bar = 10 μm, for AIE- Mito- TPP, λ_{ex} = 405 nm, λ_{em} = 450–550 nm; For PI, λ_{ex} = 543 nm, λ_{em} = 550–700 nm. SEM images of gram-positive *S. aureus* and gram-negative *E. coli* with and without AIE-Mito-TPP. [AIE-Mito-TPP] = 5μM, scale bar = 200nm. Reproduced from ref [83].

4.2. Use of AIE in AMP studies

The use of AIE fluorophores has not been extensively explored in the AMP field as yet. Here, we will discuss the few examples that have been previously reported. Li *et al* established a simple and fast method to study the interaction between the bacterial membrane and the AMP, CysHHC10[84]. CysHHC10 is a synthetic AMP that has broad-spectrum activity against both Gram-positive and Gram-negative bacteria and low induction of bacterial resistance. It has been shown to interact with the anionic bacterial surface, with a stronger interaction with Gram-positive bacteria, while exhibited a weaker affinity with Gram-negative bacterial membrane. However, even though research is ongoing on CysHHC10, there is limited knowledge on the mechanism of its antibacterial activities on the bacterial membrane[85]. Li and co-workers addressed this utilising a fluorescence technique in which CysHHC10 was conjugated with a well-known AIE probe, tetraphenylethene (TPE) (Figure 9A). After the conjugation, TPE-CysHHC10 was shown to retain its antimicrobial activity. By using flow cytometry and confocal microscopy, they showed that upon interacting with the bacterial membrane, TPE-CysHHC10 displayed intense fluorescence, indicating the cellular uptake of AIE-probe labeled AMP (Figure 9B). The toxicity levels of CysHHC10 and TPE-CysHHC10 *in vivo* is found to be negligible, suggesting CysHHC10 can be used as a potential safe therapeutic with minimal toxic side effects. TPE-CysHHC10 was further applied for visualization and localization of CysHHC10 in both the infected and normal organs *ex vivo*. However, prior to applying TPE-CysHHC10 *in vivo*, replacing TPE with a near-infrared AIE probes would be more feasible with better tissue penetration to avoid UV detection of current TPE-CysHHC10.

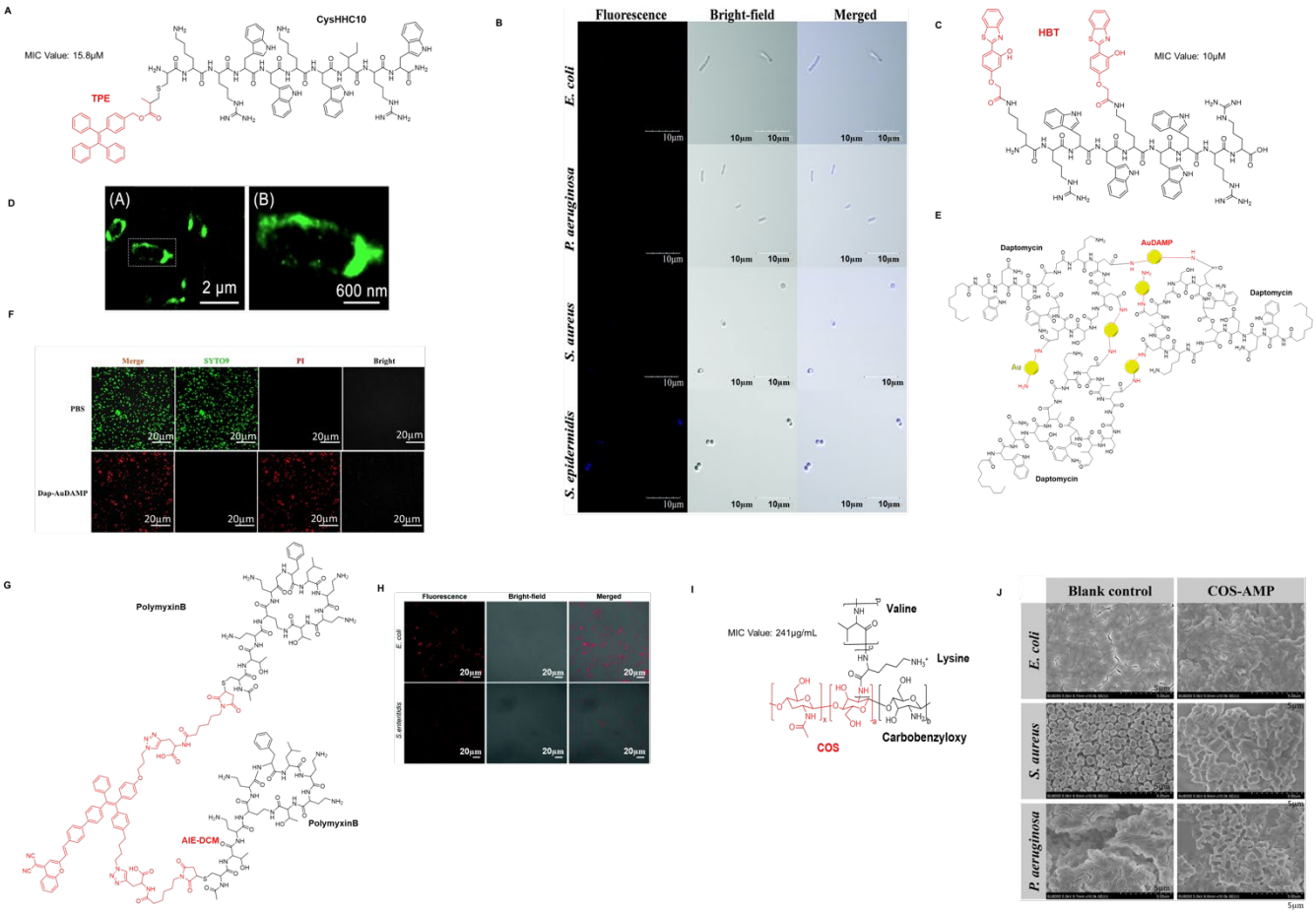

Figure 9. A) Chemical structure TPE-CysHHC10. MIC value against *E. Coli: 15.8μM.* B) CLSM images of bacteria (*E. coli*, *P. aeruginosa*, *S. aureus* and *S. epidermidis*) treated with TPE-AMP. (Reproduced from Ref. [84] with permission from The Royal Society of Chemistry.) C) Chemical structure of HBT-HHC36. MIC value against *E. coli*: 10μM. D) (A,B) Super-resolution fluorescence images of *E. coli* after treatment with AMP-2HBT. (Reprinted with permission from ref [86]. Copyright (2018) American Chemical Society.) E) Schematic illustration of Daptomycin conjugation to gold nanocluster. F) CLSM images of MRSA treated with PBS and Dap-AuDAMP at 35ºC at 1hr. The dead cells are visualised by staining red PI and viable cells are visualised by staining green SYTO 9. Reproduced by ref [87]. G) Chemical structure of AIE, DCM-polymyxin B. H) CLSM images of *E. coli and S. enteritidis* incubated with AIE-DCM-2polymyxinB. Reproduced by ref [92] with permission from The Royal Society of Chemistry. I) Chemical structure of COS-AMP. For chemical structures, Red indicates the AIE dye and black indicates the AMP. MIC value again *E. coli*: 241μg/mL. J) Cell morphology of *E. coli, S. aureus and P. aeruginosa* in blank control and with COS-AMP, Reproduced by ref [94].

Later, Chen *et al* addressed the current challenges of understanding the interaction mechanism of AMP HHC36 with bacteria by using a similar approach[86]. HHC36 displays excellent bactericidal activity for both Gram-positive and Gram-negative bacteria[88]. Although several hypotheses have been proposed, the specific mechanism of HHC36 targeting bacteria remains elusive[89]. Thus, to investigate its binding process, Chen *et al* modified HHC36 with the AIE probe, 2-(2-hydroxyphenyl) benzothiazole (HBT) to allow real-time monitoring of its localization (Figure 9C). The conjugation of HBT was found to not disturb the antibacterial activity of HHC36**.** By using AIE HBT fluorescence, they showed that the HBT-HHC36 was accumulated on the membrane surface with further disruption of the membrane structure of both Gram-positive and Gram-negative bacteria (Figure 9D). This application enhanced the perspective of AIE as an applicable probe to study the mechanism of the given AMP. It, in turn, will guide the development of more efficient and potent AMP in the antibacterial field.

Zheng and co-workers conjugated the lipopeptide antibiotic, daptomycin[90], with an antibacterial gold nanocluster, bearing intrinsic AIE properties (Figure 9E&F)[87]. Due to dual antibacterial properties of lipopeptide and gold nanocluster, the conjugates showed an enhanced synergistic antibacterial effect and faster membrane disruption by creating more and larger holes on the membrane. It was shown to eliminate bacteria within half an hour and had rapid antibacterial kinetics. The AIE property of the hybrid assisted the analysis of the lipopeptide's interaction with the bacterial wall. Different from the previous two examples that used small molecule AIE probes to conjugate with AMPs, this report demonstrated a new type of AIE fluorescence hybrid materials with its intrinsic unique properties for mechanistic investigation.

With the rapid development of AIE photosensitizers[91], dual functional AIE probes have been applied for not only visualization but also controlled killing of bacteria upon photoirradiation. In a recent example, Bao *et al* developed an AIE-polymyxin conjugate for specific detection and photodynamic killing of Gram-negative bacteria[92]. In particular, they have incorporated near-infrared AIE photosensitizer, dicyanomethylene-4H-pyran (DCM), into the polymyxin B peptide (Figure 9G&H). Due to the strong binding affinity of polymyxin B to LPS on the cell wall of the Gram-negative bacteria, it caused restriction of rotation on the AIE probe, thus allowing visualization of the cell wall and killing of bacteria upon photoactivation. This theranostic strategy allows specific detection and effective killing of Gram-negative bacteria. These results demonstrated that AIE-peptide conjugates may be used for differentiating different types of bacteria, for understanding AMP's mechanistic action on the bacterial membrane and for effective elimination of the targeted

bacteria. It is also able to provide an alternate strategy to detecting bacteria since it is able to specifically bind to LPS on the cell wall of Gram-negative bacteria[93] rather than relying on the electrostatic interaction.

The significant potential of AMPs has generated research to expand the scope to AMP-like compounds including antimicrobial polymers. Due to their similar nature to AMPs, antimicrobial polymers possess most of the advantages of AMPs with the additional merits such as the ease of scale up production, better chemical stability and low cost. Dong *et al* have developed an antimicrobial polymer based on peptidopolysaccharide, which is comprised of chitooligiosaccharide (COS) with intrinsic AIE property[94] as the core and grafting random copolymers of lysine and valine on to its amino groups (Figure 9I&J). With the aid of its AIE characteristic, COS-AMP can be used for quantitative analysis of bacteria. Upon binding to negatively charged bacteria through electrostatic interaction, it can accumulate on the bacterial surface as revealed by fluorescence microscopy and showed increased fluorescence intensity with the increase of bacteria concentration. Interestingly, COS-AMP displayed an excitation-dependent fluorescence property that allows mulit-color imaging to accommodate the settings of different microscopes and flow cytometers and enhance accurate positioning of markers. Furthermore, COS-AMP can be assembled into nanoparticles with increased antibacterial activity, which was enhanced by the plate coating method which improved its antimicrobial effect. The hybrid COS-AMP had low mammalian cell toxicity as demonstrated with above 90% cell viability in mammalian cell assays and had a low hemolytic activity. Due to its amphiphilic nature, it enhanced the COS-AMP's biocompatibility, making it a promising technique to use in clinical applications of AMP.

5. Conclusion and Perspective

Current development of AMPs in the antibacterial sector has provided a potential solution to combat AMR. Most AMPs can induce membrane-lytic processes on bacterial inner membranes with less tendency to develop resistance. With AMP development, further understanding of an AMP's mechanism, toxicity and properties are required to assist in optimizing their efficacy. To assist the future development of efficient AMPs and understand their mechanisms, we highlighted the development of fluorophores, especially AIE dyes, and their utility in antibacterial field to investigate their mode of actions in this review.

Due to the versatility and easy implementation in different biological systems, conventional organic fluorophores have been used to assist the analysis of AMPs' properties. The emergence of fluorescent materials with AIE properties offers new opportunity to overcome challenges faced by conventional fluorophores such as photostability and self-quenching. The incorporation of fluorophores into the AMPs allows the accurate localization of AMPs in biological systems. In turn, they can also be used for accurate and high-throughput quantification of the bacteria. As AIE application in AMP field is still in its early stage, we suggest several considerations need to be beard in mind for the development of novel AIE probes to determine AMP mechanism. Firstly, the AIE probes of interest should be incorporated into AMPs without deceasing their antibacterial properties. Secondly, the development of these AIE probes should exhibit compatibility with synthetic peptide procedures to ensure ease of adoption. Finally, it will shed light on the practical applications of AIE probes and AMPs. With the development and application of fluorescence technologies, advanced spectroscopy and microscopy such as super-resolution microscopy, fluorescence lifetime microscopy and fluorescence correlation spectroscopy can be used to achieve higher spatiotemporal resolution and obtain quantitative information of biomolecular interactions and dynamics to further assist to the understanding of AMP mechanism. Overall, this review provides a guide and perspective of AIE as an applicable probe for AMPs in mechanistic investigations, which in turn will assist the development of more potent antibacterial agents to combat infections.

References

[1] R. Gaynes, *Emerg. Infect. Dis.* **2017**, *23*, 849-853.
[2] C. L. Ventola, *Pharm. Ther.* **2015**, *40*, 277.
[3] W. C. Reygaert, *AIMS Microbiol.* **2018**, *4*, 482-501.
[4] S. Ebmeyer, E. Kristiansson D. G. J. Larsson, *Commun. Biol.* **2021**, *4*, 8.
[5] C. K. Shore A. Coukell, *Nat. Microbiol.* **2016**, *1*, 16083.
[6] a) in *Record number of countries contribute data revealing disturbing rates of antimicrobial resistance, Vol. 2020* World Health Organisation, **2020**; b) H. Gethun, I. Smith, K. Trivedi, S. Paulin H. H. Balkhy, *Bull. World Health Organ.* **2020**, *98*, 442-442A.
[7] J. O'Neill in *Antimicrobial resistance Vol. Tackling a crisis for the health and wealth of nations* **2014**.
[8] a) W. Li, J. Tailhades, N. O'Brien-Simpson, F. Separovic, L. Otvos, Jr., M. A. Hossain J. Wade, *Amino Acids* **2014**, *46*, 2287-2294; b) A. Peschel H.-G. Sahl, *Nat. Rev. Microbiol.* **2006**, *4*, 529.
[9] C.-F. Le, C.-M. Fang S. D. Sekaran, *Antimicrob. Agents Chemother.* **2017**, *61*, e02340-02316.
[10] a) J. Li, J.-J. Koh, S. Liu, R. Lakshminarayanan, C. S. Verma R. W. Beuerman, *Front. Neurosci.* **2017**, *11*, 73; b) M. A. Naafs, *Biomed. J. Sci. Tech. Res.* **2018**, *7*, 6038-6042; c) H. B. Koo J. Seo, *Pep. Sci.* **2019**, *111*, e24122.
[11] J. Lei, L. Sun, S. Huang, C. Zhu, P. Li, J. He, V. Mackey, D. H. Coy Q. He, *Am. J. Transl. Res.* **2019**, *7*, 3919-3931.
[12] J. L. Lau M. K. Dunn, *Bioorg. Med. Chem.* **2018**, *26*, 2700-2707.
[13] a) I. W. Hamley, *Biomacromolecules* **2014**, *15*, 1543–1559; b) R. E. W. Hancock H.-G. Sahl, *Nat. Biotechnol.* **2006**, *24*, 1551; c) Y. Shai Z. Oren, *Peptides* **2001**, *22*, 1629-1641; d) W. Li, F. Separovic, N. O'Brien-Simpson J. D. Wade, *Chem. Soc. Rev.* **2021**, doi: 10.1039/d0cs01026j.
[14] K. J. Hallock, D.-K. Lee A. Ramamoorthy, *Biophys. J.* **2003**, *84*, 3052-3060.
[15] M. Jarva, F. T. Lay, T. K. Phan, C. Humble, I. K. H. Poon, M. R. Bleackley, M. A. Anderson, M. D. Hulett M. Kvansakul, *Nat. Commun.* **2018**, *9*, 1962.
[16] J. C. Chatham S. J. Blackband, *ILAR J.* **2001**, *42*, 189-208.
[17] A. M. Davis, S. J. Teague G. J. Kleywegt, *Angew. Chem. Int. Ed.* **2003**, *42*, 2718-2736.
[18] F. Separovic, D. W. Keizer M.-A. Sani, *Front. Med. Technol.* **2020**, *2*, 610203.
[19] K. C. de Alemida, T. B. Lima, D. O. Motta, O. N. Silva, B. S. Magalhães, S. C. Dias O. L. Franco, *J. Antibiot* **2014**, *67*, 681-687.
[20] M. Mahlapuu, J. Hakansson, L. Ringstad C. Bjorn, *Front. cell. infect.* **2016**, *6*, 194.

[21] a) M. Hoyos-Nogués, F. J. Gil C. Mas-Moruno, *Molecules* **2018**, *23*, 1683; b) A. K. Buck, D. E. Elmore L. E. Darling, *Future Med. Chem.* **2019**, *11*, 2447-2460.
[22] a) M. L. Gee, M. Burton, A. Grevis-James, M. A. Hossain, S. McArthur, E. A. Palombo, J. D. Wade A. H. A. Clayton, *Sci. Rep.* **2013**, *3*, 1557; b) H. Choi, N. Rangarajan J. C. Weisshaar, *Trends Microbiol.* **2016**, *24*, 111-122.
[23] Y. Hong, J. W. Y. Lam B. Z. Tang, *Chem. Commun.* **2009**, 4332-4353.
[24] A. S. Ladokhin, W. C. Wimley S. H. White, *Biophys. J.* **1995**, *69*, 1964-1971.
[25] J. Luo, Z. Xie, J. W. Y. Lam, L. Cheng, H. Chen, C. Qiu, H. S. Kwok, X. Zhan, Y. Liu, D. Zhu B. Z. Tang, *Chem. Commun.* **2001**, 1740-1741.
[26] Y. Hong, J. W. Y. Lam B. Z. Tang, *Chem. Soc. Rev.* **2011**, *40*, 5361-5388.
[27] M. Gao B. Z. Tang, *ACS Sensors* **2017**, *2*, 1382-1399.
[28] S. Xie, A. Y. H. Wong, S. Chen B. Z. Tang, *Chem. Eur. J.* **2019**, *25*, 5824-5847.
[29] D. Wang, M. M. S. Lee, W. Xu, R. T. K. Kwok, J. W. Y. Lam B. Z. Tang, *Theranostics* **2018**, *8*, 4925-4956.
[30] a) D. Ding, K. Li, B. Liu B. Z. Tang, *Acc. Chem. Res.* **2013**, *46*, 2441-2453; b) X. Zhang, K. Wang, M. Liu, X. Zhang, L. Tao, Y. Chen Y. Wei, *Nanoscale* **2015**, *7*, 11486-11508; c) X. Zhang, B. Yao, Q. Hu, Y. Hong, A. Wallace, K. Reynolds, C. Ramsey, A. Maeder, R. Reed Y. Tang, *Mater. Chem. Front.* **2020**, *4*, 2548-2570.
[31] G. R. Steinberg D. Carling, *Nat. Rev. Drug Discov.* **2019**, *18*, 527-551.
[32] a) G. Diamond, N. Beckloff, A. Weinberg K. O. Kisich, *Curr. Pharm. Des.* **2009**, *15*, 2377-2392; b) Y. Lai R. L. Gallo, *Trends Immunol.* **2009**, *30*, 131-141.
[33] a) J. E. Lopez-Meza, A. Ochoa-Zarzosa, J. E. Barboza-Corona D. K. Bideshi, *BioMed Research International* **2015**, *2015*, 367243; b) M. Pushpanathan, P. Gunasekaran J. Rajendhran, *Int. J. Pept.* **2013**, *2013*, 15.
[34] K. Browne, S. Chakraborty, R. Chen, M. D. Willcox, D. S. Black, W. R. Walsh N. Kumar, *Int. J. Mol. Sci.* **2020**, *21*, 7047.
[35] in *Iseganan Hydrochloride in Preventing Oral Mucositis in Patients Who Are Undergoing Radiation Therapy for Head and Neck Cancer*, *Vol.* https://ClinicalTrials.gov/show/NCT00022373, **2000**.
[36] K. L. H. Lam, Y. Ishitsuka, Y. Cheng, K. Chien, A. J. Waring, R. I. Lehrer K. Y. C. Lee, *J. Phys. Chem. B* **2006**, *110*, 21282-21286.
[37] F. J. Giles, R. Redman, S. Yazji L. Bellm, *Expert Opin. Investig. Drugs* **2002**, *11*, 1161-1170.
[38] M. J. Melchers, J. Teague, P. Warn, J. Hansen, F. Bernardini, A. Wach, D. Obrecht, G. E. Dale J. W. Mouton, *Antimicrob. Agents Chemother.* **2019**, *63*.
[39] in *Study of the Effects of Brilacidin Oral Rinse on Radiation-induced Oral Mucositis in Patients With Head and Neck Cancer*, *Vol.* https://ClinicalTrials.gov/show/NCT02324335, **2014**.
[40] in *Efficacy and Safety Study of Brilacidin to Treat Serious Skin Infections*, *Vol.* https://ClinicalTrials.gov/show/NCT02052388, **2014**.
[41] G. N. Tew, R. W. Scott, M. L. Klein W. F. DeGrado, *Acc. Chem. Res.* **2010**, *43*, 30-39.
[42] B. Mensa, G. L. Howell, R. Scott W. F. DeGrado, *Antimicrob. Agents Chemother.* **2014**, *58*, 5136-5145.
[43] A. Bakovic, K. Risner, N. Bhalla, F. Alem, T. L. Chang, W. K. Weston, J. A. Harness A. Narayanan, *Viruses* **2021**, *13*, 271.
[44] J. Hakansson, L. Ringstad, A. Umerska, J. Johansson, T. Andersson, L. Boge, R. T. Rozenbaum, P. K. Sharma, P. Tollback, C. Bjorn, P. Saulnier M. Mahlapuu, *Front. cell. infect.* **2019**, *9*, 174.
[45] A. Schmidtchen, M. Pasupuleti, M. Morgelin, M. Davoudi, J. Alenfall, A. Chalupka M. Malmsten, *J. Biol. Chem.* **2009**, *284*, 17584-17594.
[46] a) J. Li in *Reviving Polymyxins: Achievements, Lessons and the Road Ahead*, Eds.: J. Li, R. L. Nation K. S. Kaye), Springer International Publishing, Cham, **2019**, pp. 1-8; b) N. Mookherjee, L. M. Rehaume R. E. W. Hancock, *Expert Opin. Ther. Targets* **2007**, *11*, 993-1004.
[47] a) Y. Engelberg M. Landau, *Nat. Commun.* **2020**, *11*, 3894; b) N. Jochumsen, R. L. Marvig, S. Damkiær, R. L. Jensen, W. Paulander, S. Molin, L. Jelsbak A. Folkesson, *Nat. Commun.* **2016**, *7*, 13002.
[48] H. X. Luong, T. T. Thanh T. H. Tran, *Life Sci.* **2020**, *260*, 118407.
[49] L. Uttley, S. Harnan, A. Cantrell, C. Taylor, M. Walshaw, K. Brownlee P. Tappenden, *Eur. Respir. Rev.* **2013**, *22*, 476-486.
[50] M. J. Mitchell, M. M. Billingsley, R. M. Haley, M. E. Wechsler, N. A. Peppas R. Langer, *Nat. Rev. Drug Discov.* **2021**, *20*, 101-124.
[51] I. d'Angelo, B. Casciaro, A. Miro, F. Quaglia, M. L. Mangoni F. Ungaro, *Colloids Surf. B Biointerfaces* **2015**, *135*, 717-725.
[52] J. Xiao, S. Chen, J. Yi, H. F. Zhang G. A. Ameer, *Adv. Funct. Mater.* **2017**, *27*, 1604872.
[53] A. Behfar, R. Crespo-Diaz, A. Terzic B. J. Gersh, *Nat. Rev. Cardiol.* **2014**, *11*, 232-246.
[54] U. H. N. Durr, U. S. Sudheendra A. Ramamoorthy, *Biochim. Biophys. Acta* **2006**, *1758*, 1408-1425.
[55] M. S. Butler, M. A. Blaskovich M. A. Cooper, *J. Antibiot.* **2013**, *66*, 571-591.
[56] S. Wang, C. Yan, X. Zhang, D. Shi, L. Chi, G. Luo J. Deng, *Biomater. Sci.* **2018**.
[57] a) L. Yan, Y. Zhang, B. Xu W. Tian, *Nanoscale* **2016**, *8*, 2471-2487; b) S. Chen, H. Wang, Y. Hong B. Z. Tang, *Mater. Horiz.* **2016**, *3*, 283-293; c) J. Yang, J. Wei, F. Luo, J. Dai, J.-J. Hu, X. Lou F. Xia, *Top. Curr. Chem.* **2020**, *378*, 47; d) Y. Zhang, Y. Wang, J. Wang X.-J. Liang, *Mater. Horiz.* **2018**, *5*, 799-812.
[58] a) E. Montesinos, *FEMS Microbiol. Lett.* **2007**, *270*, 1-11; b) E. Montesinos E. Bardaji, *Chem. Biodiversity* **2008**, *5*, 1225-1237.
[59] M. Jarosiewicz, K. Garbacz, D. Neubauer W. Kamysz, *Animals (Basel)* **2020**, *10*.
[60] B. Huerta, A. Maldonado, P. J. Ginel, C. Tarradas, L. Gómez-Gascón, R. J. Astorga I. Luque, *Vet. Microbiol.* **2011**, *150*, 302-308.
[61] K. Garbacz, S. Zarnowska, L. Piechowicz K. Haras, *Curr. Microbiol.* **2013**, *66*, 169-173.
[62] M. Rai, R. Pandit, S. Gaikwad G. Kövics, *J. Food Sci. Technol.* **2016**, *53*, 3381-3394.
[63] B. Agrillo, M. Balestrieri, M. Gogliettino, G. Palmieri, R. Moretta, Y. T. R. Proroga, I. Rea, A. Cornacchia, F. Capuano, G. Smaldone L. De Stefano, *Int. J. Mol. Sci.* **2019**, *20*, 601.
[64] A. Tanhaeian, M. Mirzaii, Z. Pirkhezranian M. H. Sekhavati, *BMC Biotechnol.* **2020**, *20*, 19.
[65] L. G. Bermudez-Humaran, C. Aubry, J.-P. Motta, C. Deraison, L. Steidler, N. Vergnolle, J.-M. Chatel P. Langella, *Curr. Opin. Microbiol.* **2013**, *16*, 278-283.
[66] K. Volzing, J. Borrero, M. J. Sadowsky Y. N. Kaznessis, *ACS Synth. Biol.* **2013**.
[67] a) L. Mendive-Tapia, C. Zhao, A. R. Akram, S. Preciado, F. Albericio, M. Lee, A. Serrels, N. Kielland, N. D. Read, R. Lavilla M. Vendrell, *Nat. Commun.* **2016**, *7*, 10940; b) W. Li, N. O'Brien-Simpson, J. Tailhades, N. Pantarat, R. Dawson, L. Otvos, Jr., E. Reynolds, F. Separovic, M. Hossain J. Wade, *Chem. Biol.* **2015**, *22*, 1250-1258.
[68] A. R. Akram, N. Avlonitis, E. Scholefield, M. Vendrell, N. McDonald, T. Aslam, T. H. Craven, C. Gray, D. S. Collie, A. J. Fisher, P. A. Corris, T. Walsh, C. Haslett, M. Bradley K. Dhaliwal, *Sci. Rep.* **2019**, *9*, 8422.
[69] B.-H. Gan, T. N. Siriwardena, S. Javor, T. Darbre J.-L. Reymond, *ACS Infect. Dis.* **2019**, *5*, 2164–2173.
[1] R. Gaynes, *Emerg. Infect. Dis.* **2017**, *23*, 849-853.
[2] C. L. Ventola, *Pharm. Ther.* **2015**, *40*, 277.
[3] W. C. Reygaert, *AIMS Microbiol.* **2018**, *4*, 482-501.
[4] S. Ebmeyer, E. Kristiansson D. G. J. Larsson, *Commun. Biol.* **2021**, *4*, 8.
[5] C. K. Shore A. Coukell, *Nat. Microbiol.* **2016**, *1*, 16083.
[6] a) in *Record number of countries contribute data revealing disturbing rates of antimicrobial resistance, Vol. 2020* World Health Organisation, **2020**; b) H. Gethun, I. Smith, K. Trivedi, S. Paulin H. H. Balkhy, *Bull. World Health Organ.* **2020**, *98*, 442-442A.
[7] J. O'Neill in *Antimicrobial resistance Vol. Tackling a crisis for the health and wealth of nations* **2014**.
[8] a) W. Li, J. Tailhades, N. O'Brien-Simpson, F. Separovic, L. Otvos, Jr., M. A. Hossain J. Wade, *Amino Acids* **2014**, *46*, 2287-2294; b) A. Peschel H.-G. Sahl, *Nat. Rev. Microbiol.* **2006**, *4*, 529.

[9] C.-F. Le, C.-M. Fang S. D. Sekaran, *Antimicrob. Agents Chemother.* **2017**, *61*, e02340-02316.
[10] a) J. Li, J.-J. Koh, S. Liu, R. Lakshminarayanan, C. S. Verma R. W. Beuerman, *Front. Neurosci.* **2017**, *11*, 73; b) M. A. Naafs, *Biomed. J. Sci. Tech. Res.* **2018**, *7*, 6038-6042; c) H. B. Koo J. Seo, *Pep. Sci.* **2019**, *111*, e24122.
[11] J. Lei, L. Sun, S. Huang, C. Zhu, P. Li, J. He, V. Mackey, D. H. Coy Q. He, *Am. J. Transl. Res.* **2019**, *7*, 3919-3931.
[12] J. L. Lau M. K. Dunn, *Bioorg. Med. Chem.* **2018**, *26*, 2700-2707.
[13] a) I. W. Hamley, *Biomacromolecules* **2014**, *15*, 1543–1559; b) R. E. W. Hancock H.-G. Sahl, *Nat. Biotechnol.* **2006**, *24*, 1551; c) Y. Shai Z. Oren, *Peptides* **2001**, *22*, 1629-1641; d) W. Li, F. Separovic, N. O'Brien-Simpson J. D. Wade, *Chem. Soc. Rev.* **2021**, doi: 10.1039/d0cs01026j.
[14] K. J. Hallock, D.-K. Lee A. Ramamoorthy, *Biophys. J.* **2003**, *84*, 3052-3060.
[15] M. Jarva, F. T. Lay, T. K. Phan, C. Humble, I. K. H. Poon, M. R. Bleackley, M. A. Anderson, M. D. Hulett M. Kvansakul, *Nat. Commun.* **2018**, *9*, 1962.
[16] J. C. Chatham S. J. Blackband, *ILAR J.* **2001**, *42*, 189-208.
[17] A. M. Davis, S. J. Teague G. J. Kleywegt, *Angew. Chem. Int. Ed.* **2003**, *42*, 2718-2736.
[18] F. Separovic, D. W. Keizer M.-A. Sani, *Front. Med. Technol.* **2020**, *2*, 610203.
[19] K. C. de Alemida, T. B. Lima, D. O. Motta, O. N. Silva, B. S. Magalhães, S. C. Dias O. L. Franco, *J. Antibiot* **2014**, *67*, 681-687.
[20] M. Mahlapuu, J. Hakansson, L. Ringstad C. Bjorn, *Front. cell. infect.* **2016**, *6*, 194.
[21] a) M. Hoyos-Nogués, F. J. Gil C. Mas-Moruno, *Molecules* **2018**, *23*, 1683; b) A. K. Buck, D. E. Elmore L. E. Darling, *Future Med. Chem.* **2019**, *11*, 2447-2460.
[22] a) M. L. Gee, M. Burton, A. Grevis-James, M. A. Hossain, S. McArthur, E. A. Palombo, J. D. Wade A. H. A. Clayton, *Sci. Rep.* **2013**, *3*, 1557; b) H. Choi, N. Rangarajan J. C. Weisshaar, *Trends Microbiol.* **2016**, *24*, 111-122.
[23] Y. Hong, J. W. Y. Lam B. Z. Tang, *Chem. Commun.* **2009**, 4332-4353.
[24] A. S. Ladokhin, W. C. Wimley S. H. White, *Biophys. J.* **1995**, *69*, 1964-1971.
[25] J. Luo, Z. Xie, J. W. Y. Lam, L. Cheng, H. Chen, C. Qiu, H. S. Kwok, X. Zhan, Y. Liu, D. Zhu B. Z. Tang, *Chem. Commun.* **2001**, 1740-1741.
[26] Y. Hong, J. W. Y. Lam B. Z. Tang, *Chem. Soc. Rev.* **2011**, *40*, 5361-5388.
[27] M. Gao B. Z. Tang, *ACS Sensors* **2017**, *2*, 1382-1399.
[28] S. Xie, A. Y. H. Wong, S. Chen B. Z. Tang, *Chem. Eur. J.* **2019**, *25*, 5824-5847.
[29] D. Wang, M. M. S. Lee, W. Xu, R. T. K. Kwok, J. W. Y. Lam B. Z. Tang, *Theranostics* **2018**, *8*, 4925-4956.
[30] a) D. Ding, K. Li, B. Liu B. Z. Tang, *Acc. Chem. Res.* **2013**, *46*, 2441-2453; b) X. Zhang, K. Wang, M. Liu, X. Zhang, L. Tao, Y. Chen Y. Wei, *Nanoscale* **2015**, *7*, 11486-11508; c) X. Zhang, B. Yao, Q. Hu, Y. Hong, A. Wallace, K. Reynolds, C. Ramsey, A. Maeder, R. Reed Y. Tang, *Mater. Chem. Front.* **2020**, *4*, 2548-2570.
[31] G. R. Steinberg D. Carling, *Nat. Rev. Drug Discov.* **2019**, *18*, 527-551.
[32] a) G. Diamond, N. Beckloff, A. Weinberg K. O. Kisich, *Curr. Pharm. Des.* **2009**, *15*, 2377-2392; b) Y. Lai R. L. Gallo, *Trends Immunol.* **2009**, *30*, 131-141.
[33] a) J. E. Lopez-Meza, A. Ochoa-Zarzosa, J. E. Barboza-Corona D. K. Bideshi, *BioMed Research International* **2015**, *2015*, 367243; b) M. Pushpanathan, P. Gunasekaran J. Rajendhran, *Int. J. Pept.* **2013**, *2013*, 15.
[34] K. Browne, S. Chakraborty, R. Chen, M. D. Willcox, D. S. Black, W. R. Walsh N. Kumar, *Int. J. Mol. Sci.* **2020**, *21*, 7047.
[35] in *Iseganan Hydrochloride in Preventing Oral Mucositis in Patients Who Are Undergoing Radiation Therapy for Head and Neck Cancer*, *Vol.* https://ClinicalTrials.gov/show/NCT00022373, **2000**.
[36] K. L. H. Lam, Y. Ishitsuka, Y. Cheng, K. Chien, A. J. Waring, R. I. Lehrer K. Y. C. Lee, *J. Phys. Chem. B* **2006**, *110*, 21282-21286.
[37] F. J. Giles, R. Redman, S. Yazji L. Bellm, *Expert Opin. Investig. Drugs* **2002**, *11*, 1161-1170.
[38] M. J. Melchers, J. Teague, P. Warn, J. Hansen, F. Bernardini, A. Wach, D. Obrecht, G. E. Dale J. W. Mouton, *Antimicrob. Agents Chemother.* **2019**, *63*.
[39] in *Study of the Effects of Brilacidin Oral Rinse on Radiation-induced Oral Mucositis in Patients With Head and Neck Cancer*, *Vol.* https://ClinicalTrials.gov/show/NCT02324335, **2014**.
[40] in *Efficacy and Safety Study of Brilacidin to Treat Serious Skin Infections*, *Vol.* https://ClinicalTrials.gov/show/NCT02052388, **2014**.
[41] G. N. Tew, R. W. Scott, M. L. Klein W. F. DeGrado, *Acc. Chem. Res.* **2010**, *43*, 30-39.
[42] B. Mensa, G. L. Howell, R. Scott W. F. DeGrado, *Antimicrob. Agents Chemother.* **2014**, *58*, 5136-5145.
[43] A. Bakovic, K. Risner, N. Bhalla, F. Alem, T. L. Chang, W. K. Weston, J. A. Harness A. Narayanan, *Viruses* **2021**, *13*, 271.
[44] J. Hakansson, L. Ringstad, A. Umerska, J. Johansson, T. Andersson, L. Boge, R. T. Rozenbaum, P. K. Sharma, P. Tollback, C. Bjorn, P. Saulnier M. Mahlapuu, *Front. cell. infect.* **2019**, *9*, 174.
[45] A. Schmidtchen, M. Pasupuleti, M. Morgelin, M. Davoudi, J. Alenfall, A. Chalupka M. Malmsten, *J. Biol. Chem.* **2009**, *284*, 17584-17594.
[46] a) J. Li in *Reviving Polymyxins: Achievements, Lessons and the Road Ahead*, Eds.: J. Li, R. L. Nation K. S. Kaye), Springer International Publishing, Cham, **2019**, pp. 1-8; b) N. Mookherjee, L. M. Rehaume R. E. W. Hancock, *Expert Opin. Ther. Targets* **2007**, *11*, 993-1004.
[47] a) Y. Engelberg M. Landau, *Nat. Commun.* **2020**, *11*, 3894; b) N. Jochumsen, R. L. Marvig, S. Damkiær, R. L. Jensen, W. Paulander, S. Molin, L. Jelsbak A. Folkesson, *Nat. Commun.* **2016**, *7*, 13002.
[48] H. X. Luong, T. T. Thanh T. H. Tran, *Life Sci.* **2020**, *260*, 118407.
[49] L. Uttley, S. Harnan, A. Cantrell, C. Taylor, M. Walshaw, K. Brownlee P. Tappenden, *Eur. Respir. Rev.* **2013**, *22*, 476-486.
[50] M. J. Mitchell, M. M. Billingsley, R. M. Haley, M. E. Wechsler, N. A. Peppas R. Langer, *Nat. Rev. Drug Discov.* **2021**, *20*, 101-124.
[51] I. d'Angelo, B. Casciaro, A. Miro, F. Quaglia, M. L. Mangoni F. Ungaro, *Colloids Surf. B Biointerfaces* **2015**, *135*, 717-725.
[52] J. Xiao, S. Chen, J. Yi, H. F. Zhang G. A. Ameer, *Adv. Funct. Mater.* **2017**, *27*, 1604872.
[53] A. Behfar, R. Crespo-Diaz, A. Terzic B. J. Gersh, *Nat. Rev. Cardiol.* **2014**, *11*, 232-246.
[54] U. H. N. Durr, U. S. Sudheendra A. Ramamoorthy, *Biochim. Biophys. Acta* **2006**, *1758*, 1408-1425.
[55] M. S. Butler, M. A. Blaskovich M. A. Cooper, *J. Antibiot.* **2013**, *66*, 571-591.
[56] S. Wang, C. Yan, X. Zhang, D. Shi, L. Chi, G. Luo J. Deng, *Biomater. Sci.* **2018**.
[57] a) L. Yan, Y. Zhang, B. Xu W. Tian, *Nanoscale* **2016**, *8*, 2471-2487; b) S. Chen, H. Wang, Y. Hong B. Z. Tang, *Mater. Horiz.* **2016**, *3*, 283-293; c) J. Yang, J. Wei, F. Luo, J. Dai, J.-J. Hu, X. Lou F. Xia, *Top. Curr. Chem.* **2020**, *378*, 47; d) Y. Zhang, Y. Wang, J. Wang X.-J. Liang, *Mater. Horiz.* **2018**, *5*, 799-812.
[58] a) E. Montesinos, *FEMS Microbiol. Lett.* **2007**, *270*, 1-11; b) E. Montesinos E. Bardaji, *Chem. Biodiversity* **2008**, *5*, 1225-1237.
[59] M. Jarosiewicz, K. Garbacz, D. Neubauer W. Kamysz, *Animals (Basel)* **2020**, *10*.
[60] B. Huerta, A. Maldonado, P. J. Ginel, C. Tarradas, L. Gómez-Gascón, R. J. Astorga I. Luque, *Vet. Microbiol.* **2011**, *150*, 302-308.
[61] K. Garbacz, S. Zarnowska, L. Piechowicz K. Haras, *Curr. Microbiol.* **2013**, *66*, 169-173.
[62] M. Rai, R. Pandit, S. Gaikwad G. Kövics, *J. Food Sci. Technol.* **2016**, *53*, 3381-3394.
[63] B. Agrillo, M. Balestrieri, M. Gogliettino, G. Palmieri, R. Moretta, Y. T. R. Proroga, I. Rea, A. Cornacchia, F. Capuano, G. Smaldone L. De Stefano, *Int. J. Mol. Sci.* **2019**, *20*, 601.
[64] A. Tanhaeian, M. Mirzaii, Z. Pirkhezranian M. H. Sekhavati, *BMC Biotechnol.* **2020**, *20*, 19.
[65] L. G. Bermudez-Humaran, C. Aubry, J.-P. Motta, C. Deraison, L. Steidler, N. Vergnolle, J.-M. Chatel P. Langella, *Curr. Opin. Microbiol.* **2013**, *16*, 278-283.
[66] K. Volzing, J. Borrero, M. J. Sadowsky Y. N. Kaznessis, *ACS Synth. Biol.* **2013**.

[67] a) L. Mendive-Tapia, C. Zhao, A. R. Akram, S. Preciado, F. Albericio, M. Lee, A. Serrels, N. Kielland, N. D. Read, R. Lavilla M. Vendrell, *Nat. Commun.* **2016**, *7*, 10940; b) W. Li, N. O'Brien-Simpson, J. Tailhades, N. Pantarat, R. Dawson, L. Otvos, Jr., E. Reynolds, F. Separovic, M. Hossain J. Wade, *Chem. Biol.* **2015**, *22*, 1250-1258.
[68] A. R. Akram, N. Avlonitis, E. Scholefield, M. Vendrell, N. McDonald, T. Aslam, T. H. Craven, C. Gray, D. S. Collie, A. J. Fisher, P. A. Corris, T. Walsh, C. Haslett, M. Bradley K. Dhaliwal, *Sci. Rep.* **2019**, *9*, 8422.
[69] B.-H. Gan, T. N. Siriwardena, S. Javor, T. Darbre J.-L. Reymond, *ACS Infect. Dis.* **2019**, *5*, 2164–2173.
[70] a) W. Li, N. M. O'Brien-Simpson, S. Yao, J. Tailhades, E. C. Reynolds, R. M. Dawson, L. Otvos, M. A. Hossain, F. Separovic J. D. Wade, *Chem. Eur. J.* **2017**, *23*, 390-396; b) W. Li, M.-A. Sani, E. Jamasbi, L. Otvos Jr, M. A. Hossain, J. D. Wade F. Separovic, *Biochim. Biophys. Acta* **2016**, *1858*, 1236-1243.
[71] L. Smith, M. Kohli A. M. Smith, *J. Am. Chem. Soc.* **2018**, *140*, 13904-13912.
[72] a) X. Cai B. Liu, *Angew. Chem. Int. Ed.* **2020**, *59*, 9868-9886; b) Y. Wang, J. Nie, W. Fang, L. Yang, Q. Hu, Z. Wang, J. Z. Sun B. Z. Tang, *Chem. Rev.* **2020**, *120*, 4534-4577.
[73] R. Hu, N. L. C. Leung B. Z. Tang, *Chem. Soc. Rev.* **2014**, *43*, 4494-4562.
[74] a) J. Mei, N. L. C. Leung, R. T. K. Kwok, J. W. Y. Lam B. Z. Tang, *Chem. Rev.* **2015**, *115*, 11718-11940; b) K. Zhang, J. Shu, W. Chu, X. Liu, B. Xu W. Jiang, *Dyes Pigm.* **2021**, *185*, 108898.
[75] H. Bai, W. He, J. H. C. Chau, Z. Zheng, R. T. K. Kwok, J. W. Y. Lam B. Z. Tang, *Biomaterials* **2021**, *268*, 120598.
[76] K. Li, W. Qin, D. Ding, N. Tomczak, J. Geng, R. Liu, J. Liu, X. Zhang, H. Liu, B. Liu B. Z. Tang, *Sci. Rep.* **2013**, *3*, 1150.
[77] a) J. K. Jaiswal, E. R. Goldman, H. Mattoussi S. M. Simon, *Nat. Methods* **2004**, *1*, 73-78; b) B. S. Shah, P. A. Clark, E. K. Moioli, M. A. Stroscio J. J. Mao, *Nano Lett.* **2007**, *7*, 3071-3079.
[78] Z. Sheng, B. Guo, D. Hu, S. Xu, W. Wu, W. H. Liew, K. Yao, J. Jiang, C. Liu, H. Zheng B. Liu, *Adv. Mater. (Weinheim, Ger.)* **2018**, *30*, 1800766.
[79] a) A. L. Antaris, H. Chen, K. Cheng, Y. Sun, G. Hong, C. Qu, S. Diao, Z. Deng, X. Hu, B. Zhang, X. Zhang, O. K. Yaghi, Z. R. Alamparambil, X. Hong, Z. Cheng H. Dai, *Nat. Mater.* **2016**, *15*, 235-242; b) C. Li, L. Cao, Y. Zhang, P. Yi, M. Wang, B. Tan, Z. Deng, D. Wu Q. Wang, *Small* **2015**, *11*, 4517-4525.
[80] a) X. Dang, L. Gu, J. Qi, S. Correa, G. Zhang, A. M. Belcher P. T. Hammond, *Proc. Natl. Acad. Sci. U. S. A.* **2016**, *113*, 5179-5184; b) G. Hong, Y. Zou, A. L. Antaris, S. Diao, D. Wu, K. Cheng, X. Zhang, C. Chen, B. Liu, Y. He, J. Z. Wu, J. Yuan, B. Zhang, Z. Tao, C. Fukunaga H. Dai, *Nat. Commun.* **2014**, *5*, 4206.
[81] a) L. Han, D. K. Kong, M.-q. Zheng, S. Murikinati, C. Ma, P. Yuan, L. Li, D. Tian, Q. Cai, C. Ye, D. Holden, J.-H. Park, X. Gao, J.-L. Thomas, J. Grutzendler, R. E. Carson, Y. Huang, J. M. Piepmeier J. Zhou, *ACS Nano* **2016**, *10*, 4209-4218; b) Z. Tao, G. Hong, C. Shinji, C. Chen, S. Diao, A. L. Antaris, B. Zhang, Y. Zou H. Dai, *Angew. Chem. Int. Ed.* **2013**, *52*, 13002-13006.
[82] J. Yang, J. Dai, Q. Wang, Y. Cheng, J. Guo, Z. Zhao, Y. Hong, X. Lou F. Xia, *Angew. Chem. Int. Ed.* **2020**, *59*, 20405-20410.
[83] X. Chen, L. Huang, Y. Jia, R. Hu, M. Gao, L. Ren B. Z. Tang, *Advanced Optical Materials* **2020**, *8*, 1902191.
[84] N. N. Li, J. Z. Li, P. Liu, D. Pranantyo, L. Luo, J. C. Chen, E.-T. Kang, X. F. Hu, C. M. Li L. Q. Xu, *Chem. Commun.* **2017**, *53*, 3315-3318.
[85] K. A. Brogden, *Nat. Rev. Microbiol.* **2005**, *3*, 238-250.
[86] J. Chen, M. Gao, L. Wang, S. Li, J. He, A. Qin, L. Ren, Y. Wang B. Z. Tang, *ACS Appl. Mater. Interfaces* **2018**, *10*, 11436-11442.
[87] Y. Zheng, W. Liu, Y. Chen, C. Li, H. Jiang X. Wang, *J. Colloid Interface Sci.* **2019**, *546*, 1-10.
[88] M. Nichols, M. Kuljanin, M. Nategholeslam, T. Hoang, S. Vafaei, B. Tomberli, C. G. Gray, L. DeBruin M. Jelokhani-Niaraki, *J. Phys. Chem. B* **2013**, *117*, 14697-14708.
[89] M. Nategholeslam, S. Vafaei, M. Nichols, M. Kuljanin, M. Jelokhani-Niaraki, B. Tomberli C. G. Gray, *Biophys. J.* **2012**, *102*, 397a-398a.
[90] R. M. Humphries, S. Pollett G. Sakoulas, *Clin. Microbiol. Rev.* **2013**, *26*, 759-780.
[91] J. Dai, X. Wu, S. Ding, X. Lou, F. Xia, S. Wang Y. Hong, *J. Med. Chem.* **2020**, *63*, 1996-2012.
[92] P. Bao, C. Li, H. Ou, S. Ji, Y. Chen, J. Gao, X. Yue, J. Shen D. Ding, *Biomater. Sci.* **2021**, *9*, 437-442.
[93] M. P. McInerney, K. D. Roberts, P. E. Thompson, J. Li, R. L. Nation, T. Velkov J. A. Nicolazzo, *J. Pharm. Sci.* **2016**, *105*, 1006-1010.
[94] Z. Dong, Y. Wang, C. Wang, H. Meng, Y. Li C. Wang, *Adv. Healthc. Mater.* **2020**, *9*, 2000419.